

Tuning spin-torque nano-oscillator nonlinearity using He^+ irradiation

Sheng Jiang,^{1,2} Roman Khymyn,² Sunjae Chung,^{1,3} Quang Tuan Le,^{1,2} Liza Herrera Diez,⁴ Afshin Houshang,^{2,5} Mohammad Zahedinejad,² Dafiné Ravelosona,^{4,6} and Johan Åkerman^{1,2,5,*}

¹*Department of Applied Physics, School of Engineering Sciences,
KTH Royal Institute of Technology, Electrum 229, SE-16440 Kista, Sweden*

²*Department of Physics, University of Gothenburg, 412 96, Gothenburg, Sweden*

³*Department of Physics and Astronomy, Uppsala University, 751 20 Uppsala, Sweden*

⁴*Institut d'Electronique Fondamentale, CNRS, Université Paris-Sud, Université Paris-Saclay, 91405 Orsay, France*

⁵*NanOsc AB, Kista 164 40, Sweden*

⁶*Spin-Ion Technologies, 28 rue du Général Leclerc, 78000 Versailles Cedex, France*

(Dated: March 16, 2022)

We use He^+ irradiation to tune the nonlinearity, \mathcal{N} , of all-perpendicular spin-torque nano-oscillators (STNOs) using the He^+ fluence-dependent perpendicular magnetic anisotropy (PMA) of the [Co/Ni] free layer. Employing fluences from 6 to $20 \times 10^{14} \text{ He}^+/\text{cm}^2$, we are able to tune \mathcal{N} in an in-plane field from strongly positive to moderately negative. As the STNO microwave signal properties are mainly governed by \mathcal{N} , we can in this way directly control the threshold current, the current tunability of the frequency, and the STNO linewidth. In particular, we can dramatically improve the latter by more than two orders of magnitude. Our results are in good agreement with the theory for nonlinear auto-oscillators, confirm theoretical predictions of the role of nonlinearity, and demonstrate a straightforward path towards improving the microwave properties of STNOs.

DOI: XXXXXX.

Spin-torque nano-oscillators (STNOs) are among the most promising candidates for nanoscale broadband microwave generators [1–6] and detectors [7–9]. STNOs can generate broadband microwave frequencies ranging from hundreds of MHz to the sub-THz [10–12], controlled by both magnetic fields and dc currents [5, 13]. Moreover, the device size can be reduced to a few tens of nanometers, which is of great opportunity for industrial applications. They can also host a range of novel magnetodynamical spin wave modes, such as propagating spin waves of different orders [14, 15], and magnetodynamical solitons, such as spin wave bullets [14] and droplets [3].

However, the applicability of these devices has suffered from their low power emission and large linewidth. Nonlinear auto-oscillator theory [16–19] explains the large linewidth as a result of the strong nonlinearity \mathcal{N} , *i.e.* the dependence of the microwave frequency on its precession amplitude. \mathcal{N} can be controlled not only by the measurement conditions [13, 20–24], such as the magnitude and direction of the magnetic field, but also by the magnetic properties of the free layer of the STNO, such as the magnetic anisotropy and the effective magnetization [19]. For instance, in an easy-plane free layer, \mathcal{N} changes gradually from positive to negative values as the direction of magnetic field rotates from out-of-plane to in-plane [16, 19]. Experimental studies have corroborated [13, 14, 16, 21, 25–27] this theoretical prediction, as the linewidth shows a minimum when \mathcal{N} crosses zero at the critical field angle. This suggests a way to improve the linewidth by selectively reducing the nonlinearity.

Whereas all previous studies aimed at minimizing the nonlinearity have focused only on the effects of the external conditions in single devices, a more general and prac-

tical solution should be based on the intrinsic magnetic properties of the device itself. In our work, we therefore study systematically how \mathcal{N} is affected by the strength of perpendicular magnetic anisotropy (PMA) H_k in a set of nanocontact (NC) STNOs. We show how \mathcal{N} can be continuously tuned as H_k is controlled by He^+ irradiation fluence [28–31] in otherwise identical devices. Most importantly, the linewidth is dramatically improved at moderate H_k values, where $\mathcal{N} \rightarrow 0$. Finally, we show excellent agreement of our experimental results with nonlinear auto-oscillator theory [19].

The STNO devices were fabricated from all-perpendicular (all-PMA) [Co/Pd]/Cu/[Co/Ni] [32, 33] and orthogonal [Co/Pd]/Cu/NiFe spin valves (SVs). The full stack consists of a Ta (5)/Cu (15)/Ta (5)/Pd (3) seed layer, an all-PMA [Co (0.5)/Pd (1.0)] \times 5/Cu (7)/[Co (0.3)/Ni (0.9)] \times 4/Co (0.3) or orthogonal [Co (0.5)/Pd (1.0)] \times 5/Cu (7)/Ni₈₀Fe₂₀ (4.5) SV with a Cu(3)/Pd(3) capping layer, sputtered onto a thermally oxidized 100 mm Si wafer (numbers in parentheses are layer thicknesses in nanometers). The deposited stacks were first patterned into $8 \mu\text{m} \times 20 \mu\text{m}$ mesas using photolithography and ion-milling etching, followed by chemical vapor deposition (CVD) of an insulating 40-nm-thick SiO₂ film. Electron beam lithography and reactive ion etching were used to open nanocontacts (with nominal radius of R_{NC} 35 nm) through the SiO₂ in the center of each mesa. The processed wafer was then cut into different pieces for He^+ irradiation with the fluence F varied from 6 to $20 \times 10^{14} \text{ He}^+/\text{cm}^2$ [33]. Fabrication was completed with lift-off lithography and deposition of a Cu (500 nm)/Au (100 nm) top electrode in a single run with all irradiated pieces. Our protocol hence en-

TABLE I. Sample structure information and the calculated effective magnetization $\mu_0 M_{\text{eff}}$ of free layer ([Co/Ni] or NiFe) for various He^+ -irradiation fluences. $\mu_0 M_{\text{eff}}$ are measured by ST-FMR (see the supplemental materials [41]).

Structure	Fluence ($\times 10^{14} \text{ He}^+/\text{cm}^2$)	$\mu_0 M_{\text{eff}}$ (T)
[Co/Pd]/Cu/[Co/Ni]	0	-0.68
[Co/Pd]/Cu/[Co/Ni]	6	-0.44
[Co/Pd]/Cu/[Co/Ni]	10	-0.14
[Co/Pd]/Cu/[Co/Ni]	20	0.03
[Co/Pd]/Cu/NiFe	-	0.98

tures that all other properties, except the He^+ fluence, are identical from device to device.

We used our custom-built probe station for static and microwave characterization. A direct current I_{dc} was injected into the devices using a Keithley 6221 current source, and the dc voltage was detected using a Keithley 2182 nanovoltmeter. The magnetic field was applied in the plane of the film. The generated microwave signals from the STNO device were decoupled from the dc voltage via a bias-tee, amplified using a low-noise amplifier, and then recorded with a spectrum analyzer [34, 35].

To accurately determine M_{eff} of the [Co/Ni] free layer, spin-torque ferromagnetic resonance (ST-FMR) [36–40] measurements were performed on the He^+ -irradiated STNOs (see details in supplemental materials [41]). The fluence information and the obtained effective magnetization $\mu_0 M_{\text{eff}}$ are presented in Table I. The value of M_{eff} (H_k) increases (decreases) as the fluence increases. Here, the NiFe free layer is used as a reference for a larger M_{eff} sample.

In Fig. 1, we compare the calculated FMR frequency, f_{FMR} , using the measured M_{eff} , with the microwave signals generated from the STNO devices. The inset in Fig. 1 shows a typical power spectral density (PSD) of the microwave signals for a fluence of $F = 10 \times 10^{14} \text{ He}^+/\text{cm}^2$. All PSD spectra are well fitted with a Lorentz function, and the extracted frequency f versus magnetic field is presented in Fig. 1 with different symbols for each different fluence. All data show a quasi-linear dependence on the magnetic field, and the generated microwave frequency f extends to lower values as M_{eff} (H_k) increases (decreases). This behavior is consistent with the calculated value of the FMR frequency f_{FMR} , plotted as dashed lines in Fig. 1. The overall trends of f_{FMR} are in good agreement with the auto-oscillation f . The difference between the calculated f_{FMR} and the measured auto-oscillation f is a direct measure of the nonlinearity of the magnetization precession [5, 14, 23, 42], which is discussed in detail below.

We now turn to the current-induced frequency tunability. Figures 2(a)–2(e) show the generated microwave frequency f versus dc current I_{dc} at a fixed magnetic field, $\mu_0 H = 0.72 \text{ T}$; f linearly depends on the I_{dc} at different

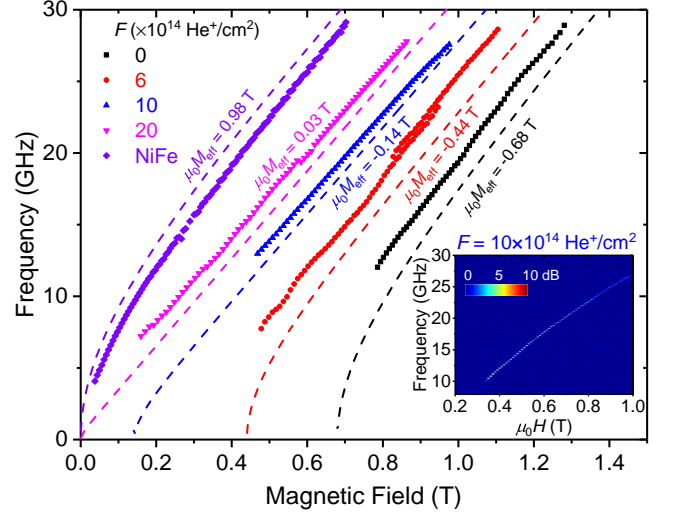


FIG. 1. Auto-oscillation frequency versus in-plane magnetic field for various irradiated STNOs with $R_{\text{NC}} = 35 \text{ nm}$. The dashed lines are the calculated FMR frequencies f_{FMR} , based on the values of $\mu_0 M_{\text{eff}}$ obtained from ST-FMR measurements [41]. Inset: A typical power spectral density (PSD) of an STNO with $F = 10 \times 10^{14} \text{ He}^+/\text{cm}^2$ at $I_{\text{dc}} = -14 \text{ mA}$.

values of M_{eff} . The current-induced frequency tunability df/dI_{dc} can be extracted from the slopes of linear fits which plot as each dashed line in Figs. 2(a)–2(e). df/dI_{dc} for M_{eff} are then summarized in Fig. 2(f). We found that *i*) df/dI_{dc} decreases from 0.50 GHz/mA for nonirradiated [Co/Ni] to -0.13 GHz/mA for NiFe as M_{eff} increases (or H_k decreases), *ii*) the sign of df/dI_{dc} changes from positive (for [Co/Ni]) to negative (for NiFe), consistent with the easy axis transition from out-of-plane for [Co/Ni] to in-plane for NiFe, and further details will be discussed later.

We carried out detailed measurements at different magnetic fields to understand further the behavior of df/dI_{dc} . Figure 3(a) shows one example of extracted f versus I_{dc} at different fields, ranging from 0.37 to 1.12 T with a 0.05 T step, for $F = 6 \times 10^{14} \text{ He}^+/\text{cm}^2$. All data show clear linear dependencies on I_{dc} . Here we would like to define one numerical relation about the tunability, $df/d\zeta = I_{\text{th}}(df/dI_{\text{dc}})$, to compare our experimental results directly with theoretical calculation, where $\zeta = I_{\text{dc}}/I_{\text{th}}$ is the dimensionless supercriticality parameter [19] and I_{th} is the threshold current. I_{th} were extracted from plots of inverse power $1/P$ versus I_{dc} as described in supplemental materials [41]. After obtained all I_{th} and df/dI_{dc} for different M_{eff} , $df/d\zeta$ are represented as solid dots in Fig. 3(b). All $df/d\zeta$ for different M_{eff} show similar behaviors that is inverse proportional to magnetic field. It is noteworthy that the overall $df/d\zeta$ decreases as M_{eff} (H_k) increases (decreases). It reaches around zero when the $\mu_0 M_{\text{eff}} \approx 0$ for $F = 20 \times 10^{14} \text{ He}^+/\text{cm}^2$. The sign of $df/d\zeta$ for NiFe is even negative.

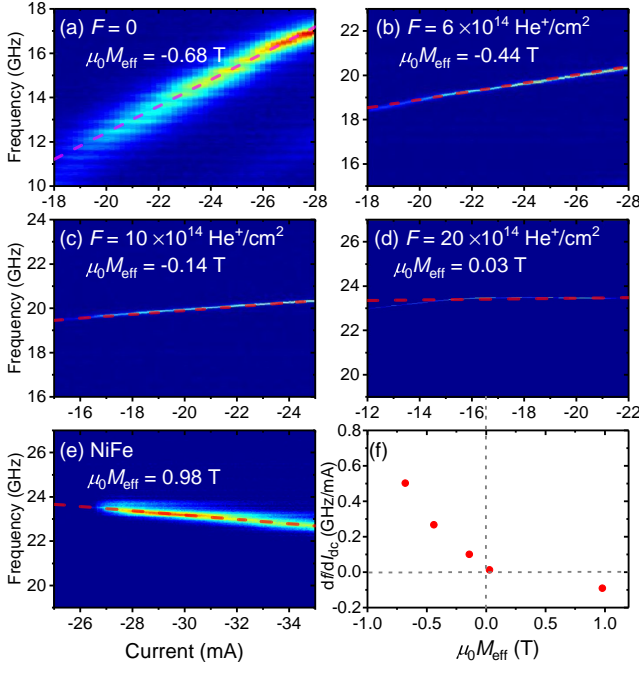


FIG. 2. (a)–(e) PSD versus I_{dc} in STNOs with different irradiated fluences at $\mu_0 H = 0.72$ T. The red dotted line represents the linear fits of the auto-oscillation frequency. (f) slope df/dI_{dc} versus $\mu_0 M_{eff}$ extracted from the fits of (a)–(e).

To understand the behavior of tunability versus M_{eff} (H_k) from He⁺-irradiated STNOs, we considered the nonlinear auto-oscillator theory of A. Slavin and V. Tiberkevich [18, 19, 42, 43], which was derived from universal auto-oscillation systems and has proved to be consistent with the Landau–Lifshitz–Gilbert–Slonczewski (LLGS) equation [19]. This theory allows us to describe the experimental observation analytically. The auto-oscillation frequency f generated from an STNO is expressed as:

$$f(I_{dc}) = f_{FMR} + \frac{\mathcal{N}}{2\pi} \frac{\zeta - 1}{\zeta + Q}, \quad (1)$$

where \mathcal{N} is the nonlinearity factor, $\frac{\zeta - 1}{\zeta + Q} = P_0$ is the normalized power of the stationary precession, and Q is the nonlinear damping coefficient. From Eq. (1), the frequency shift is mainly decided by the nonlinearity \mathcal{N} . Taking the derivation of Eq. (1), $df/d\zeta$ is derived as:

$$\frac{df}{d\zeta} = I_{th} \frac{df}{dI_{dc}} = \frac{\mathcal{N}}{2\pi} \frac{1 + Q}{(\zeta + Q)^2}. \quad (2)$$

The nonlinear frequency shift coefficient \mathcal{N} for STNOs dominates the frequency tunability, and may be positive, zero, or negative, depending on magnetic field direction and magnetic anisotropy of free layer in STNOs.

To explain the experimental observations using this analytical theory, we derive \mathcal{N} with our experimental con-

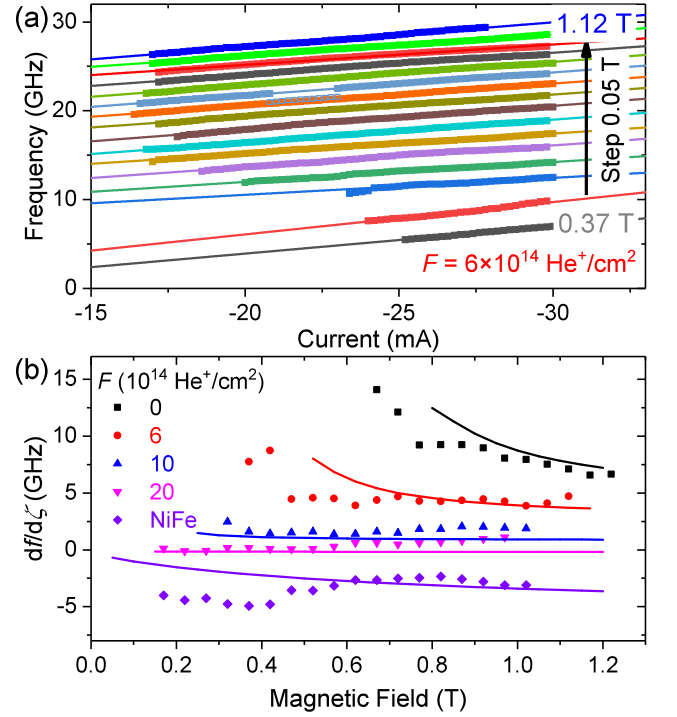


FIG. 3. (a) Extracted auto-oscillation frequency f vs. I_{dc} at different magnetic fields for $F = 6 \times 10^{14}$ He⁺/cm². Some minor frequency jumps at $\mu_0 H = 0.87$ T are shown as rectangular boxes, possibly due to film inhomogeneities generating different dynamical behaviors. (b) $df/d\zeta$ [*i.e.* $I_{th}(df/dI_{dc})$] vs. magnetic field, where I_{th} is extracted from the intercept of the inverse power of the auto-oscillation signals and the df/dI_{dc} are the slopes of the linear fits of frequency as $I_{dc} > I_{th}$ (see supplemental materials [41]). The solid lines are the theoretical calculation from Eqs. (2)–(4).

ditions. The nonlinearity is expressed as [42]

$$\mathcal{N} = -\frac{\omega_H \omega_M (\omega_H + \omega_M/4)}{\omega_0 (\omega_H + \omega_M/2)}, \quad (3)$$

$$\begin{cases} \omega_H = \gamma H \\ \omega_M = 4\pi\gamma M_{eff} \\ \omega_0 = \gamma \sqrt{\omega_H (\omega_H + \omega_M)}. \end{cases} \quad (4)$$

We note that Eqs. (3) and (4) are valid for the magnetization of the free layer being aligned to the magnetic field direction. Utilizing Eqs. (3) and (4), we calculate $df/d\zeta$ ($\propto \mathcal{N}$), where ζ and Q are used as fitting parameters for all data in Fig. 3(b), and we find reasonable good agreements with 1.5 for ζ and 3.0 for Q , respectively. All calculated results are shown as the solid lines alongside the experimental results in Fig. 3(b). It should be noted that the theoretical calculation coincides with experimental results in the overall trend, although there are discrepancies between experiment and theory. One reason for these discrepancies is likely that the theory does not take into account the current-induced Joule heating

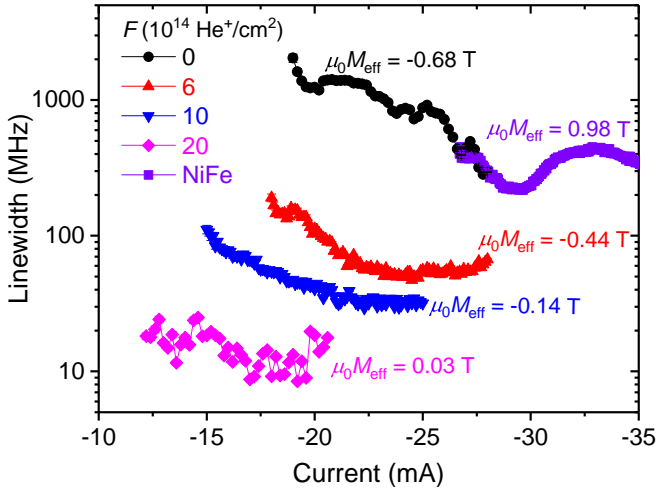


FIG. 4. Linewidth Δf versus I_{dc} with different effective magnetization $\mu_0 M_{eff}$ at $\mu_0 H = 0.72$ T. The linewidth were extracted from the data in Figs. 3(a)–3(e).

and Oersted fields that are present in the experiments. In addition, the calculated nonlinearity \mathcal{N} can also explain the frequency difference between the calculated f_{FMR} and the generated microwave frequency f in Fig. 1. Due to the negative value of \mathcal{N} (or $df/d\zeta$) for NiFe, f is expected to be lower than f_{FMR} , as predicted in Eq. (1) and consistent with our experimental observations in Fig. 1. This auto-oscillation mode is often characterized as a localized bullet [13, 14, 42]. In contrast, \mathcal{N} is positive for easy out-of-plane [Co/Ni], so $f > f_{FMR}$ in Fig. 1 [13, 32, 42]. In this case, its mode favors to be a propagating spin-wave [13, 27, 44]. All of these experimental observations confirm the theoretical predictions very well.

Furthermore, according to nonlinear auto-oscillator theory, the linewidth Δf of the generated microwave signals can be expressed as [19]

$$\Delta f = \Gamma_+(P_0) \frac{k_B T}{E(P_0)} \left[1 + \left(\frac{\mathcal{N}}{\Gamma_{eff}} \right)^2 \right], \quad (5)$$

where k_B is the Boltzmann constant and T is the temperature. $\Gamma_+(P_0)$ and $E(P_0)$ are the damping function and time-averaged oscillation energy as a function of the power P_0 , respectively. Γ_{eff} is the effective damping. In Eq.(5), the linewidth Δf exhibits a quadratic dependence on the nonlinearity \mathcal{N} . To compare with our experimental results, we extracted the linewidth from the data in Figs. 2(a)–2(e), as shown in Fig. 4. The linewidth was indeed dramatically improved by two orders of magnitude as \mathcal{N} decreases (as M_{eff} increases), it reaches to a lowest value for $\mu_0 M_{eff} = 0.03$ T where $\mathcal{N} \rightarrow 0$. Δf again increases for the NiFe free layer when \mathcal{N} becomes moderately negative. The excellent agreement between our experimental results and theory confirms that the linewidth can be minimized intentionally by controlling the nonlinearity in general, and tuning it to zero in par-

ticular. When the PMA compensates the demagnetization field, the nonlinearity identically equals zero regardless of the external conditions. We can therefore minimize the linewidth by choosing free layer materials with $\mu_0 M_{eff} \rightarrow 0$. We hence would emphasize that our study can offers a universal path to solving one of the key issues in utilizing STNOs as microwave generators. As for the generated microwave power—another key drawback of this type of microwave generators—we did not observe an improvement in this study, mainly due to the slightly degradation in magnetoresistance (MR) values [33]. We expect that the power can be dramatically improved using magnetic tunnel junction-based STNOs, whose MR can be over two orders of magnitude greater than that of spin valve-based STNOs. [2, 15].

In conclusion, we have presented a systematic study of the variation of nonlinearity against PMA in STNOs. By using He^+ irradiation to continuously tune the PMA of the [Co/Ni] free layer, the nonlinearity \mathcal{N} (along with the frequency tunability df/dI_{dc}) shows a continuous decreasing trend as H_k (M_{eff}) decreases (increases). As a consequence of this decreasing nonlinearity, we have achieved an approximately hundredfold improvement in the linewidth. Our experimental observations are in excellent agreement with nonlinear auto-oscillator theory. This systematic study not only verifies the theoretical prediction, but also offers a route to improving the linewidth, which is of great importance for commercializing microwave generators.

This work was supported by the China Scholarship Council (CSC), the Swedish Foundation for Strategic Research (SSF), the Swedish Research Council (VR), and the Knut and Alice Wallenberg Foundation (KAW). Additional support for the work was provided by the European Research Council (ERC) under the European Community’s Seventh Framework Programme (FP/2007-2013)/ERC Grant 307144 “MUSTANG”.

* Author to johan.akerman@physics.gu.se

- [1] A. M. Deac, A. Fukushima, H. Kubota, H. Maehara, Y. Suzuki, S. Yuasa, Y. Nagamine, K. Tsunekawa, D. D. Djayaprawira, and N. Watanabe, *Nat. Phys.* **4**, 803 (2008).
- [2] H. Maehara, H. Kubota, Y. Suzuki, T. Seki, K. Nishimura, Y. Nagamine, K. Tsunekawa, A. Fukushima, A. M. Deac, K. Ando, and S. Yuasa, *Appl. Phys. Express* **6**, 113005 (2013).
- [3] S. M. Mohseni, S. R. Sani, J. Persson, T. N. A. Nguyen, S. Chung, Y. Pogoryelov, P. K. Muduli, E. Iacocca, A. Eklund, R. K. Dumas, S. Bonetti, A. Deac, M. A. Hoefer, and J. Åkerman, *Science* **339**, 1295 (2013).
- [4] H. Maehara, H. Kubota, Y. Suzuki, T. Seki, K. Nishimura, Y. Nagamine, K. Tsunekawa, A. Fukushima, H. Arai, T. Taniguchi, H. Imamura, K. Ando, and S. Yuasa, *Appl. Phys. Express* **7**, 023003 (2014).

- (2014).
- [5] T. Chen, R. K. Dumas, A. Eklund, P. K. Muduli, A. Houshang, A. A. Awad, P. Durrenfeld, B. G. Malm, A. Rusu, and J. Åkerman, *Proc. IEEE* **104**, 1919 (2016).
 - [6] S. A. H. Banuazizi, S. R. Sani, A. Eklund, M. M. Naiini, S. M. Mohseni, S. Chung, P. Dürrenfeld, B. G. Malm, and J. Åkerman, *Nanoscale* **9**, 1896 (2017).
 - [7] P. M. Braganca, B. A. Gurney, B. A. Wilson, J. A. Kattine, S. Maat, and J. R. Childress, *Nanotechnology* **21**, 235202 (2010).
 - [8] S. Miwa, S. Ishibashi, H. Tomita, T. Nozaki, E. Tamura, K. Ando, N. Mizuochi, T. Saruya, H. Kubota, K. Yakushiji, T. Taniguchi, H. Imamura, A. Fukushima, S. Yuasa, and Y. Suzuki, *Nat. Mater.* **13**, 50 (2014).
 - [9] B. Fang, M. Carpentieri, X. Hao, H. Jiang, J. A. Kattine, I. N. Krivorotov, B. Ocker, J. Langer, K. L. Wang, B. Zhang, B. Azzerboni, P. K. Amiri, G. Finocchio, and Z. Zeng, *Nat. Commun.* **7**, 11259 (2016).
 - [10] V. S. Pribiag, I. N. Krivorotov, G. D. Fuchs, P. M. Braganca, O. Ozatay, J. C. Sankey, D. C. Ralph, and R. A. Buhrman, *Nat. Phys.* **3**, 498 (2007).
 - [11] M. Hofer, M. Ablowitz, B. Ilan, M. Pufall, and T. Silva, *Phys. Rev. Lett.* **95**, 267206 (2005).
 - [12] R. L. Stamps, S. Breitkreutz, J. Åkerman, A. V. Chumak, Y. Otani, G. E. W. Bauer, J.-U. Thiele, M. Bowen, S. A. Majetich, M. Kläui, I. L. Prejbeanu, B. Dieny, N. M. Dempsey, and B. Hillebrands, *J. Phys. D: Appl. Phys.* **47**, 333001 (2014).
 - [13] R. K. Dumas, E. Iacocca, S. Bonetti, S. R. Sani, S. M. Mohseni, A. Eklund, J. Persson, O. Heinonen, and J. Åkerman, *Phys. Rev. Lett.* **110**, 257202 (2013).
 - [14] S. Bonetti, V. Tiberkevich, G. Consolo, G. Finocchio, P. Muduli, F. Mancoff, A. Slavin, and J. Åkerman, *Phys. Rev. Lett.* **105**, 217204 (2010).
 - [15] A. Houshang, R. Khymyn, M. Dvornik, M. Haidar, S. R. Etesami, R. Ferreira, P. P. Freitas, R. K. Dumas, and J. Åkerman, *Nat. Commun.* **9**, 4374 (2018).
 - [16] J.-V. Kim, V. Tiberkevich, and A. N. Slavin, *Phys. Rev. Lett.* **100**, 017207 (2008).
 - [17] J. V. Kim, Q. Mistral, C. Chappert, V. S. Tiberkevich, and A. N. Slavin, *Phys. Rev. Lett.* **100**, 1 (2008).
 - [18] A. Slavin and V. Tiberkevich, *IEEE Trans. Magn.* **44**, 1916 (2008).
 - [19] A. Slavin and V. Tiberkevich, *IEEE Trans. Magn.* **45**, 1875 (2009).
 - [20] M. Pufall, W. Rippard, S. Russek, S. Kaka, and J. Kattine, *Phys. Rev. Lett.* **97**, 087206 (2006).
 - [21] W. H. Rippard, M. R. Pufall, and S. E. Russek, *Phys. Rev. B* **74**, 224409 (2006).
 - [22] G. Gerhart, E. Bankowski, G. A. Melkov, V. S. Tiberkevich, and A. N. Slavin, *Phys. Rev. B* **76**, 024437 (2007).
 - [23] G. Consolo, B. Azzerboni, L. Lopez-Diaz, G. Gerhart, E. Bankowski, V. Tiberkevich, and A. Slavin, *Phys. Rev. B* **78**, 014420 (2008).
 - [24] P. K. Muduli, Y. Pogoryelov, S. Bonetti, G. Consolo, F. Mancoff, and J. Åkerman, *Phys. Rev. B* **81**, 140408 (2010).
 - [25] S. Bonetti, V. Puliafito, G. Consolo, V. S. Tiberkevich, A. N. Slavin, and J. Åkerman, *Phys. Rev. B* **85**, 174427 (2012).
 - [26] O. Lee, P. Braganca, V. Pribiag, D. Ralph, and R. Buhrman, *Phys. Rev. B* **88**, 224411 (2013).
 - [27] M. Mohseni, M. Hamdi, H. F. Yazdi, S. A. H. Banuazizi, S. Chung, S. R. Sani, J. Åkerman, and M. Mohseni, *Phys. Rev. B* **97**, 184402 (2018).
 - [28] C. Chappert, H. Bernas, J. Ferre, V. Kottler, J.-P. Jamet, Y. Chen, E. Cambril, T. Devolder, F. Rousseaux, V. Mathet, and H. Launois, *Science* **280**, 1919 (1998).
 - [29] J. Fassbender, D. Ravelosona, and Y. Samson, *J. Phys. D: Appl. Phys.* **37**, R179 (2004).
 - [30] J.-M. Beaujour, D. Ravelosona, I. Tudosa, E. Fullerton, and A. D. Kent, *Phys. Rev. B* **80**, 180415 (2009).
 - [31] L. Herrera Diez, F. García-Sánchez, J.-P. Adam, T. Devolder, S. Eimer, M. S. El Hadri, A. Lamperti, R. Mantovan, B. Ocker, and D. Ravelosona, *Appl. Phys. Lett.* **107**, 032401 (2015).
 - [32] S. Chung, Q. T. Le, M. Ahlberg, A. A. Awad, M. Weigand, I. Bykova, R. Khymyn, M. Dvornik, H. Mazraati, A. Houshang, S. Jiang, T. N. A. Nguyen, E. Goering, G. Schütz, J. Gräfe, and J. Åkerman, *Phys. Rev. Lett.* **120**, 217204 (2018).
 - [33] S. Jiang, S. Chung, L. H. Diez, T. Q. Le, F. Magnusson, D. Ravelosona, and J. Åkerman, *AIP Adv.* **8**, 065309 (2018).
 - [34] S. Jiang, S. R. Etesami, S. Chung, Q. T. Le, A. Houshang, and J. Åkerman, *IEEE Magn. Lett.* **9**, 3104304 (2018).
 - [35] S. Jiang, S. Chung, Q. T. Le, H. Mazraati, A. Houshang, and J. Åkerman, *Phys. Rev. Appl.* **10**, 054014 (2018).
 - [36] Y. Okutomi, K. Miyake, M. Doi, H. N. Fuke, H. Iwasaki, and M. Sashiki, *J. Appl. Phys.* **109**, 07C727 (2011).
 - [37] L. Liu, C.-F. Pai, Y. Li, H. W. Tseng, D. C. Ralph, and R. A. Buhrman, *Science* **336**, 555 (2012).
 - [38] M. Fazlali, M. Dvornik, E. Iacocca, P. Dürrenfeld, M. Haidar, J. Åkerman, and R. K. Dumas, *Phys. Rev. B* **93**, 134427 (2016).
 - [39] H. Mazraati, S. Chung, A. Houshang, M. Dvornik, L. Piazza, F. Qejvanaj, S. Jiang, T. Q. Le, J. Weissenrieder, and J. Åkerman, *Appl. Phys. Lett.* **109**, 242402 (2016).
 - [40] M. Zahedinejad, H. Mazraati, H. Fulara, J. Yue, S. Jiang, A. A. Awad, and J. Åkerman, *Appl. Phys. Lett.* **112**, 132404 (2018).
 - [41] See supplemental material for more information.
 - [42] A. Slavin and V. Tiberkevich, *Phys. Rev. Lett.* **95**, 237201 (2005).
 - [43] A. N. Slavin and P. Kabos, *IEEE Trans. Magn.* **41**, 1264 (2005).
 - [44] M. Madami, E. Iacocca, S. Sani, G. Gubbiotti, S. Tacchi, R. K. Dumas, J. Åkerman, and G. Carlotti, *Phys. Rev. B* **92**, 024403 (2015).